depends on unfolding of a collagen fibril that can become rate-limiting. The activation energy for fibril digestion (101 kcal mol^{-1}) was found to be 4 times that of a helical collagen monomer (*26*). The high energy of activation for collagenolysis is in good agreement, however, with the apparent energy of activation for collagen fibril unfolding (124 kcal mol^{-1}) measured more recently (*27*).

We thus conclude that the MMP-1–collagen system is a Brownian ratchet that is able to rectify Brownian forces into a propulsion mechanism by coupling to collagen proteolysis. The minimum power of 1.7×10^{-19} W per molecule of MMP-1 is required to propel the enzyme along the collagen fibril with the velocity $V = 4.5 \pm 0.36$ μm s^{-1}, which was calculated from the diffusion coefficient measured experimentally (*15*). A maximum power input for the directional transport of MMP-1 at room temperature (P_C = 10%) of 1.1×10^{-18} W per molecule of MMP-1 was calculated from the assumption of 5 kcal/mol of free energy for a cleaved peptide bond (*15*). The efficiency of the motor at room temperature can then be calculated as the ratio of power output over input to be 15% (*28*). These numbers are expected to change as the value of P_C increases with rise of the temperature.

The biological consequences of the collagenase motor activity are of great interest. We hypothesize that the collagenase ratchet can serve as a clutch mechanism, assisting cell locomotion on collagen matrices and contraction of collagen gels in three-dimensional cultures. Association of the enzyme with cell membranes via interaction with tissue-specific integrins can couple the extracellular proteolysis with the forces exerted by the cytoskeleton to direct membrane protrusions along a "no-skid" surface generated by the digestion of collagen fibrils. Membrane-type MMPs (*29*, *30*) can potentially act in a similar fashion. Experimental observations that clearly demonstrate the requirement of MMP-1–dependent collagenolysis for migration of keratinocytes on collagen support this hypothesis (*31*).

References and Notes

1. T. Vu, Z. Werb, *Genes Dev.* **14**, 2123 (2000).
2. M. Egeblad, Z. Werb, *Nature Rev. Cancer* **2**, 161 (2002).
3. K. E. Kadler, D. F. Holmes, J. A. Trotter, J. A. Chapman, *Biochem. J.* **316**, 1 (1996).
4. R. Visse, H. Nagase, *Circ. Res.* **92**, 827 (2003).
5. G. I. Goldberg *et al.*, *J. Biol. Chem.* **261**, 6600 (1986).
6. G. Fields, H. Van Wart, H. Birkedal-Hansen, *J. Biol. Chem.* **262**, 6221 (1987).
7. R. P. Feynman, R. B. Leighton, M. Sands, *The Feynman Lectures on Physics* (Addison-Wesley. Reading, MA, 1966), vol. 1.
8. R. D. Astumian, *Science* **276**, 917 (1997).
9. F. Jülicher, A. Ajdari, J. Prost, *Rev. Mod. Phys.* **69**, 1269 (1997).
10. C. Peskin, G. Odell, G. Oster, *Biophys. J.* **65**, 316 (1993).
11. J. Prost, J. F. Chauwin, L. Peliti, A. Ajdari, *Phys. Rev. Lett.* **72**, 2652 (1994).
12. R. F. Fox, *Phys. Rev. E* **57**, 2177 (1998).
13. J. Mai, I. M. Sokolov, A. Blumen, *Phys. Rev. E.* **64**, 011102 (2001).
14. J. Torbet, M. Ronziere, *Biochem. J.* **219**, 1057 (1984).
15. Materials and methods are available as supporting material on *Science* Online.
16. S. Saffarian, E. L. Elson, *Biophys. J.* **84**, 2030 (2003).
17. D. Magde, E. L. Elson, W. W. Webb, *Biopolymers* **17**, 361 (1978).
18. M. Schliwa, G. Woehlke, *Nature* **422**, 759 (2003).
19. R. D. Vale, R. A. Milligan, *Science* **288**, 88 (2000).
20. H. Qian, *Biophys. Chem.* **83**, 35 (2000).
21. L. J. Windsor, M. K. Bodden, B. Birkedal-Hansen, J. A. Engler, H. Birkedal-Hansen, *J. Biol. Chem.* **269**, 26201 (1994).
22. D. L. Steele *et al.*, *Protein Eng.* **13**, 397 (2000).
23. I. E. Collier, S. Saffarian, B. L. Marmer, E. L. Elson, G. Goldberg, *Biophys. J.* **81**, 2370 (2001).
24. S. Saffarian, I. E. Collier, B. L. Marmer, E. L. Elson, G. Goldberg, unpublished observations.
25. J. J. Jeffrey, H. G. Welgus, R. Burgeson, A. Eisen, *J. Biol. Chem.* **258**, 11123 (1983).
26. H. Welgus, J. Jeffrey, G. Stricklin, W. Roswit, A. Eisen, *J. Biol. Chem.* **255**, 6806 (1980).
27. E. Leikina, M. V. Mertts, N. Kuznetsova, S. Leikin, *Proc. Natl. Acad. Sci. U.S.A.* **99**, 1314 (2002).
28. I. Derényi, M. Bier, R. D. Astumian, *Phys. Rev. Lett.* **83**, 903 (1999).
29. T. Shimada *et al.*, *Eur. J. Biochem.* **262**, 907 (1999).
30. E. Ohuchi *et al.*, *J. Biol. Chem.* **272**, 2446 (1997).
31. B. K. Pilcher *et al.*, *J. Cell Biol.* **137**, 1445 (1997).

32. The authors would like to thank M. S. Conrady for the use of the superconducting magnet. We also thank H. Qian and A. Eisen for reading the manuscript and helpful discussions. This work was supported in part by NIH grants GM-38838 to E.L.E., AR40618, AR39472 to G.I.G. and Washington University-Pfizer Inc. agreement.

Supporting Online Material

www.sciencemag.org/cgi/content/full/306/5693/108/DC1
Materials and Methods
SOM Text
Figs. S1 and S2
Tables S1 to S3
References and Notes

15 April 2004; accepted 5 August 2004

Life History Trade-Offs Assemble Ecological Guilds

Michael B. Bonsall,[1]*† Vincent A. A. Jansen,[2]* Michael P. Hassell[1]

Ecological theory predicts that competition for a limiting resource will lead to the exclusion of species unless the within-species effects outweigh the between-species effects. Understanding how multiple competitors might coexist on a single resource has focused on the prescriptive formalism of a necessary niche width and limiting similarity. Here, we show how continuously varying life histories and trade-offs in these characteristics can allow multiple competitors to coexist, and we reveal how limiting similarity emerges and is shaped by the ecological and evolutionary characteristics of competitors. In this way, we illustrate how the interplay of ecological and evolutionary processes acts to shape ecological communities in a unique way. This leads us to argue that evolutionary processes (life-history trait trade-offs) are fundamental to the understanding of the structure of ecological communities.

Ecological theory predicts that species in ecological communities can coexist only if there are differences in their responses to limiting resources (*1*, *2*). Evolutionary processes underpin this coexistence: Differences between species arise through the combined effects of selection and life-history trade-offs. Trade-offs in life histories (*3*, *4*) prevent species from evolving as Darwinian "demons" (species that develop rapidly, reproduce continuously, and do not age). Sanctioning investment in life-history characteristics against ecological competitive ability has the potential to allow multiple species to coexist by reducing the probability that any one species is demonic in an assemblage (*5*–*9*). Reducing the dominance of any one species in an assemblage and fostering equivalence among species has the potential to allow ecological diversity to be promoted (*10*, *11*).

Here, we explore the hypothesis that communities are assembled or shaped through evolutionary processes and that diversity is maintained and generated through species equivalence. Using a continuously varying strategy set, we evaluate the role of assembly and trade-offs as mechanisms for the formation of complex predator-prey assemblages. We consider a generic interaction between a class of natural enemies (parasitoids) competing for a limiting host resource (*12*, *13*). We assume that n types of consumer can attack particular juvenile (larval) stages of the host and that there is no a priori partitioning of this resource class. We describe the interaction between competing parasitoids within a generation with a system of differential equations. Solutions to these equations provide a description of the population dynamics of the system from which (ecological) difference equations (*14*) can be derived. Finally, the invasion and replacement

[1]Department of Biological Sciences, Imperial College London, Silwood Park Campus, Ascot, Berkshire SL5 7PY, UK. [2]School of Biological Sciences, Royal Holloway University of London, Egham, Surrey TW20 0EX, UK.

*These authors contributed equally to this work.
†To whom correspondence should be addressed. E-mail: m.bonsall@imperial.ac.uk

(evolutionary) dynamics can be explored from knowledge of both the competitive interaction and population dynamics.

We partition the host population into three classes: susceptible host larvae, singly parasitized larvae susceptible to further attack, and parasitized larvae not susceptible to further attack. We do this for n different strains of competing parasitoids. Parasitoids are time-limited with a finite amount of time to locate hosts, and per unit of time each parasitoid of type i discovers a host larva and lays an egg on or in it with a rate of α_i per host. Once oviposition has occurred, the parasitized host passes through a phase in which it is susceptible to further attack either by conspecifics (superparasitism events) or heterospecifics (multiparasitism events). This period of susceptibility lasts on average μ time units. This second egg will hatch and win in competition within the host with probability π_{ij}, where i denotes the type of the first parasitoid and j the type of the second. Obviously, if the same type superparasitizes a host, a parasitoid of that type will emerge. The model gives rise to a system of equations that can be solved to give the number of hosts that are parasitized and the number of consumers that arise at the beginning of the next season (*15*).

We assume that there is a trade-off between competitive ability and a life-history characteristic (*3*, *4*), in particular parasitoid attack rate (α) or parasitoid longevity ($1/c$). A parasitoid that is better at discovering new hosts (higher α) is worse at outcompeting or defending a host that is attacked (by a heterospecific) (*16*). When we use this trade-off, we assume that parasitoid death rates are the same for all parasitoids ($c_i = c$). The second trade-off that we consider is between parasitoid longevity and competitive ability (*5*, *9*). With this trade-off, it is the longer lived species that are inferior competitors. When we use this trade-off function, we assume that the potential for parasitoids to discover hosts is equivalent for all species ($\alpha_i = \alpha$). Competitive ability is always a function of the resident and invading parasitoid life-history strategies and is a characteristic determined by the ecological and evolutionary dynamics of the assemblage.

The population dynamics of the host and parasitoids (H', P'_i) over the seasons can be described by the following system of difference equations:

$$H' = f[H, x(T)] \quad (1)$$

$$P'_i = H[y_i(T) + z_i(T)] \quad (2)$$

Here, $f[H, x(T)]$ is the function relating hosts in the current season to those at the start of the next season, and within this function $x(T)$ is the probability that hosts survive parasitism. For simplicity, host density (H) is kept constant from season to season [but see (*15*) for results using variable host densities]. The functions $y_i(T)$ and $z_i(T)$ are the respective probabilities of a host being singly and doubly parasitized and producing a parasitoid of type i (*15*).

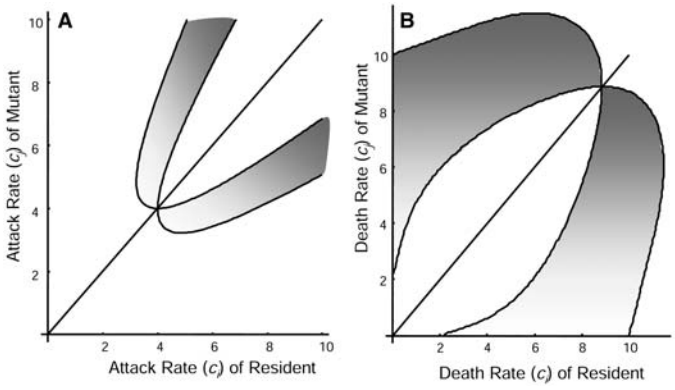

Fig. 1. Regions of coexistence (shaded areas) for the parasitoid competition model for trade-offs in (**A**) fecundity (H = 10, μ = 1.0, c = 0.5, and T = 10) and (**B**) longevity (death rate) (H = 10, μ = 1.0, α = 1.0, and T = 10). Coexistence is promoted if the mutant strategy has a higher fecundity or lower death rate compared with that of the resident. The more dissimilar two strategies are, the more likely coexistence is between competing parasitoids. These plots can also be used to infer the replacement dynamics of different strains. If the region under the diagonal is negative and the opposite region above the diagonal is positive, this will result in a strain with a marginally higher value of trait replacing the resident. If the sign pattern is opposite, then a strain with a marginally lower value of the trait will invade and outcompete the resident. Repeated appearance of slightly different strains (mutants) will result in an evolutionary change of the trait. The invasion boundaries were evaluated using a root-solving algorithm and numerical integration of the model (*15*).

To understand how different life-history characteristics affect the coexistence of competing parasitoids, we derive a set of invasion conditions. That is, for successful invasion of a second parasitoid P_j (characterized by its death rate c_j or attack rate α_j) into a population in which a parasitoid P_i (characterized by c_i or α_i) is already present, we evaluate whether P_j can invade, when rare, a population consisting of only P_i at equilibrium. The precise conditions for invasion can be derived from the rate that a rare parasitoid invades a persistent resident host–parasitoid interaction. The invasibility conditions (*15*, *17*) can be illustrated graphically in a pairwise invasibility plot (*18*, *19*) and can be analyzed using tools from game theory and adaptive dynamics. Here, rather than focusing solely on this type of dynamic, we examine what factors influence the assembly of parasitoids into guilds [closely related species that share similar life-history characteristics (*20*, *21*)] and under what conditions these guilds cannot be invaded by further species (*7*, *22*).

Mutual invasibility and coexistence of natural enemies is possible if there are differences in searching efficiency such that the inferior competitor has the higher attack rate (Fig. 1A). Similarly, Fig. 1B shows combinations of resident and invader parasitoid death rates (c) that permit coexistence under fixed host densities. Mutual invasibility and hence coexistence of parasitoids can occur only if there are distinct differences in life histories (fecundity or longevity); for example, as an inferior larval competitor, the invading parasitoid must have a lower adult death rate (or live longer) than the resident parasitoid (Fig. 1B). However, transient coexistence is possible if invading parasitoids are almost identical to the residents, because the fitness differences will be very small and the effects of competition will be almost neutral.

It is important to note from Fig. 1 (see also fig. S1) that any two combinations of strategies taken from the shaded area can coexist. However, subsequent episodes of invasion and replacement will impose a particular dynamic on the coexisting pair, and this could either result in the eventual loss of one of the strategies or introduce additional species to the assemblage. We used numerical simulations to study the dynamics of the assemblage and find its stable composition. This final assemblage is not just the assemblage in which the largest number of species can coexist. In all of the cases, the number of species in the final assemblage is larger than one but is always less than the number of species that could potentially coexist.

Numerical exploration illustrates that the invasion and dynamics of multiple parasitoids on a single limiting host resource gives rise to multiple coexisting species. However, this prediction is dependent on the abundance of the host. When host abundance is low, a dimorphism arises and two parasitoid strategies coexist (Fig. 2A). When host abundance is high, a polymorphism arises and multiple parasitoid strategies coexist (Fig. 2B). Throughout, it is assumed that new strategies are similar to existing residents, as would be the case if new variants are created through mutation in a polygenic trait. Evolutionary branching leads to a number of coexisting distinct types. Within each broad group, several closely related parasitoid types compete intensely for dominance and assemble into clades. These assemblages arise as a result of the interplay between evolutionary and ecological processes: This is not encountered in conventional studies, which solely concentrate on the ecological processes of coexistence (*8*, *23*–*26*). For instance, the oc-

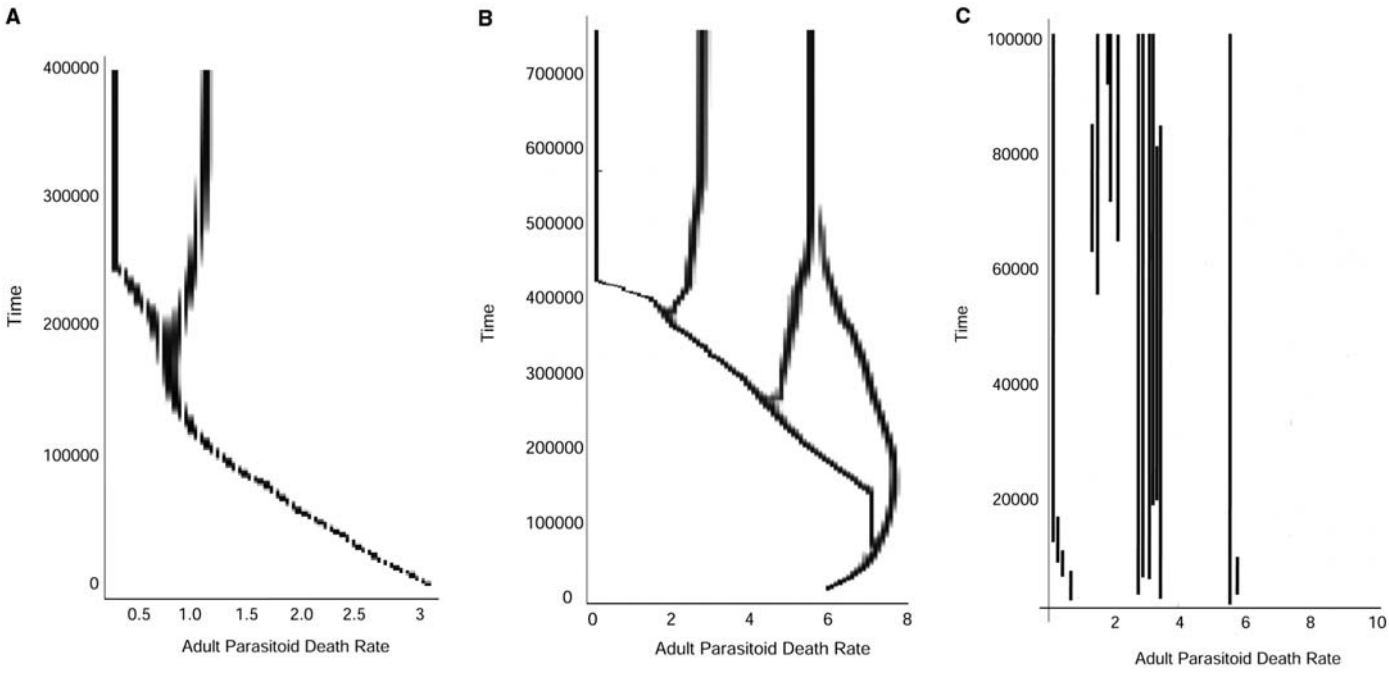

Fig. 2. Branching pattern and community assembly under (**A**) a fixed initial strategy under low host density ($H = 4$, $\mu = 1.0$, $\alpha = 1.0$, and $T = 10$), (**B**) a fixed strategy under high host density ($H = 10$, $\mu = 1.0$, $\alpha = 1.0$, and $T = 10$), and (**C**) a variety of initial strategies under trade-offs in longevity (death rate) and competitive ability ($H = 10$, $\mu = 1.0$, $\alpha = 1.0$, and $T = 10$). Limiting similarity between groups [in (A) and (B)] arises as a consequence of the population and evolutionary dynamics among competing species. In (C), transitory dynamics underpinned the interaction between similar species. Between the groups, competition is skewed, with longer lived species experiencing severe interspecific effects.

currence of this type of polymorphism can lead to reproductive isolation and speciation through sympatric mechanisms (*27*, *28*).

However, the formation of clades through evolution need not necessarily be the only mechanism by which species assembly occurs. When guilds are formed through random assembly, we find the same qualitative patterns of niche differentiation. This is demonstrated in Fig. 2C, in which new immigrants arrive as migrants from a species pool. Although guilds assembled this way converge to the same final assemblage as in Fig. 2B, there are some notable differences. In particular, the coexistence of many types is manifest. However, there are numerous unsuccessful invasions. A striking phenomenon in the assembly of species guilds is that invading strategies may persist as transients at low abundance for very long periods of time. Note that the number of different types that can coexist ecologically exceeds the number observed in the final evolutionary stable assemblage. The coexistence of multiple strategies gives rise to a form of limiting similarity with a minimum distance between each group (Fig. 2C). The competition between different types is highly asymmetric, such that long-lived strategies are subjected to greater effects of interspecific competition than are short-lived strategies or that higher fecund strategies are subjected to stronger interspecific competition than are less fecund strategies; then, the observed evolutionary stable coexistence arises as a result of distinct differences in life history. The degree of competition between similar species is intense and almost symmetric.

Unlike earlier theoretical studies (*1–2*, *29–31*), this limiting similarity between strategy sets arises as a consequence of the population and evolutionary dynamics of the trophic interaction rather than as a result of a prescriptive statistical relationship derived from the shape of the competition function (*1*, *2*). It is expected that locally coexisting species should be less similar than one would expect by chance alone. However, across similar life-history strategies a number of species contest for dominance through intense interspecific competition. Given that over appropriate time scales species are observed to coexist, we conjecture that coexisting species may be more similar than one would expect by chance alone and that their distribution falls into a number of distinct life-history class clusters. Difference in resource use will depend on species demographic and life-history characteristics.

These properties (the emergence of niche structures, limiting similarity, and transient coexistence) are likely to hold for a large class of competitive interactions (*15*) (fig. S2). Our generic result that is not limited to predator-prey interactions is that ecological and evolutionary dynamics of resource-consumer interactions shape the structure of species assemblages (*15*). In contrast to conventional theory on trade-offs and community assembly (*32*), which predict no limit to diversity (because any species can occupy any point in trait space), we show that species life-history trade-offs can generate a limiting similarity that promotes ecological diversity. Evolutionary and ecological dynamical processes drive niche partitioning and limiting similarity, and at the same time generate diversity within a niche. While the total size of different niches is determined by competition for a set of limited resources, the relative abundance of strains within a niche is determined predominantly by chance (*33*). Our approach reconciles two conflicting views about the organization of ecological communities: organization dominated by niche structure (*29–31*) and organization through chance and neutral processes (*10*, *11*). These two views are not mutually exclusive. Both processes operate simultaneously to generate and maintain diversity in ecological communities.

References and Notes

1. R. H. MacArthur, R. Levins, *Am. Nat.* **101**, 377 (1967).
2. R. M. May, *Stability and Complexity in Model Ecosystems* (Princeton Univ. Press, Princeton, NJ, 1974).
3. S. C. Stearns, *The Evolution of Life Histories* (Oxford Univ. Press, Oxford, 1992).
4. D. A. Roff, *The Evolution of Life Histories: Theory and Analysis* (Chapman & Hall, New York, 1992).
5. R. Levins, D. Culver, *Proc. Natl. Acad. Sci. U.S.A.* **68**, 1246 (1971).
6. D. Tilman, *Ecology* **75**, 2 (1994).
7. V. A. A. Jansen, G. S. E. E. Mulder, *Ecol. Lett.* **2**, 379 (1999).
8. M. B. Bonsall, M. P. Hassell, G. Asefa, *Ecology* **83**, 925 (2002).
9. M. B. Bonsall, M. Mangel, *Proc. R. Soc. Lond. B. Biol. Sci.* **271**, 1143 (2004).
10. G. Bell, *Am. Nat.* **155**, 606 (2000).
11. S. P. Hubbell, *The Unified Theory of Biodiversity and Biogeography* (Princeton Univ. Press, Princeton, NJ, 2001).
12. M. P. Hassell, *The Dynamics of Arthropod Predator-Prey Systems* (Princeton Univ. Press, Princeton, NJ, 1978).

13. M. P. Hassell, *The Temporal and Spatial Dynamics of Host-Parasitoid Associations* (Oxford Univ. Press, Oxford, 2000).
14. A. J. Nicholson, V. A. Bailey, *Proc. Zoo. Soc. Lond.* **3**, 551 (1935).
15. Materials and methods are available as supporting material on *Science* Online.
16. R. M. May, M. P. Hassell, *Am. Nat.* **117**, 234 (1981).
17. R. A. Armstrong, R. McGehee, *Am. Nat.* **115**, 151 (1980).
18. J. A. J. Metz, R. M. Nisbet, S. A. H. Geritz, *Trends Ecol. Evol.* **7**, 198 (1992).
19. S. A. H. Geritz, E. Kisdi, G. Meszena, J. A. J. Metz, *Evol. Ecol.* **12**, 35 (1998).
20. R. B. Root, *Ecol. Monogr.* **37**, 317 (1967).
21. P. Morin, *Community Ecology* (Blackwell Science, Oxford, 1999).
22. U. Dieckmann, *Trends Ecol. Evol.* **12**, 128 (1997).
23. B. R. Levin, *Evolution* **25**, 249 (1971).
24. J. Haigh, J. Maynard-Smith, *Theor. Popul. Biol.* **3**, 290 (1972).
25. F. M. Stewart, B. R. Levin, *Am. Nat.* **107**, 171 (1973).
26. C. J. Briggs, *Am. Nat.* **141**, 372 (1993).
27. U. Dieckmann, M. Doebeli, *Nature* **400**, 354 (1999).
28. M. Doebeli, U. Dieckmann, *Nature* **421**, 259 (2003).
29. G. E. Hutchinson, *Am. Nat.* **93**, 145 (1959).
30. P. A. Abrams, *Theor. Popul. Biol.* **8**, 356 (1975).
31. D. Lack, *Darwin's Finches* (Cambridge University Press, Cambridge, 1947).
32. D. Tilman, *Resource Competition and Community Structure* (Princeton Univ. Press, Princeton, NJ, 1982).
33. D. Tilman, *Proc. Natl. Acad. Sci. U.S.A.* **101**, 10854 (2004).
34. M.B.B. is a Royal Society University Research Fellow.

Supporting Online Material
www.sciencemag.org/cgi/content/full/306/5693/111/DC1
SOM Text
Figs. S1 and S2
References

25 May 2004; accepted 11 August 2004

Zebrafish Dpr2 Inhibits Mesoderm Induction by Promoting Degradation of Nodal Receptors

Lixia Zhang,[1]* Hu Zhou,[2]* Ying Su,[1]* Zhihui Sun,[1] Haiwen Zhang,[1] Long Zhang,[2] Yu Zhang,[1] Yuanheng Ning,[2] Ye-Guang Chen,[2]† Anming Meng[1]†

Nodal proteins, members of the transforming growth factor–β (TGFβ) superfamily, have been identified as key endogenous mesoderm inducers in vertebrates. Precise control of Nodal signaling is essential for normal development of embryos. Here, we report that zebrafish *dapper2* (*dpr2*) is expressed in mesoderm precursors during early embryogenesis and is positively regulated by Nodal signals. In vivo functional studies in zebrafish suggest that Dpr2 suppresses mesoderm induction activities of Nodal signaling. Dpr2 is localized in late endosomes, binds to the TGFβ receptors ALK5 and ALK4, and accelerates lysosomal degradation of these receptors.

Genetic studies have revealed that Nodal proteins are essential for mesoderm induction in vertebrates (*1*–*4*). So far, few factors have been found to inhibit Nodal signaling during early embryogenesis. Lefty proteins inhibit Nodal activity by competing for binding to their common receptors (*5*–*8*). An extracellular protein, Cerberus, binds to Nodal and blocks its activity (*9*). Tomoregulin-1, a transmembrane protein, blocks Nodal signaling by interacting with the Nodal coreceptor Cripto (*10*). Drap1 interacts with and inhibits DNA binding of FoxH1, a transcription factor that mediates Nodal signaling (*11*). Here, we demonstrate that Dpr2 inhibits Nodal signaling in zebrafish embryos, targeting Nodal receptors for lysosomal degradation.

Zebrafish *dpr2* was identified by a whole-mount in situ hybridization screen for tissue-specific genes. The putative Dpr2 protein, 837 residues long, has overall sequence identity of 30 and 36% to the putative human DAPPER1 and DAPPER2 proteins (*12*), respectively, with higher similarity in several domains (fig. S1). Several *dpr2* ESTs have been mapped adjacent to the *oprm1* and *smoc2* loci in the zebrafish linkage group 13 (LG13), a region syntenic to the human *DAPPER2* locus, which suggests that zebrafish *dpr2* is an ortholog of human *DAPPER2*. Although *Xenopus* Dapper and Frodo are almost identical, Dapper is apparently a general Dishevelled antagonist (*13*), whereas Frodo is a positive regulator of Wnt signaling (*14*).

Whole-mount in situ hybridization revealed a specific expression pattern of *dpr2* during zebrafish embryogenesis (fig. S2). It was first expressed on the dorsal blastoderm at the sphere stage, about 4 hours postfertilization (hpf). At the onset of gastrulation, *dpr2* expression was restricted to the whole germ ring where mesoderm precursors reside, with the highest expression in the embryonic shield. The *dpr2*-positive cells then involute and converge during gastrulation and thus contribute to the formation of epiblast and hypoblast. When segmentation starts, *dpr2* is expressed in the dorsal trunk neural tube, the lateral plate mesoderm, and the tail bud. At 24 hpf, *dpr2* expression is restricted to blood progenitors and the tail bud. This expression pattern of *dpr2* suggests a role in early mesoderm induction.

To study the function of *dpr2*, endogenous expression of *dpr2* was knocked down by injecting a mix of two specific and equally effective antisense morpholinos (dpr2-MOs) (fig. S3). The injected embryos generally showed a thicker, curled down trunk at 24 hpf (fig. S3), a phenotype also observed with a *lefty1* morpholino (lft1-MO) (*15*). The majority (53 to 95%) of morpholino-injected embryos showed increased expression of the organizer-specific marker *gsc* (Fig. 1A), the lateral mesodermal marker *snail1* (Fig. 1B), and the axial mesodermal markers *no tail* (*ntl*) (Fig. 1C) and *shh* (Fig. 1D). Mutations of the *oep* locus, which encodes a coreceptor for the Nodal ligands *squint* (*sqt*) and *cyclops* (*cyc*) in zebrafish, give rise to reduced Nodal activity (*4*, *16*). Overexpression of *dpr2* caused partial or complete fusion of the eyes (Fig. 1F), resembling the *oep* (Fig. 1G) and *cyc* phenotypes, which also result from insufficient Nodal signaling (*16*, *17*). Overexpression also caused partial loss of the notochord and tail reduction in about one-third of the embryos at 24 hpf. Injection of *dpr2* mRNA also led to reduction or elimination of *shh* expression at 24 hpf (Fig. 1H), as well as decreased *ntl* expression at the bud stage (fig. S3). These data suggest that *dpr2* functions to inhibit mesoderm formation.

Because *dpr2* overexpression phenocopied *oep* mutants and because *dpr2* knockdown resulted in morphological changes that resembled *lefty1* knockdown, there may be genetic interactions between Dpr2 and Nodal signaling. We found that 55% (38 out of 69) of embryos coinjected with dpr2-MOs and 0.1 pg *sqt* mRNA had a much wider notochord, an effect not seen in embryos injected with *sqt* mRNA alone (fig. S4). This notochord effect showed that knockdown of *dpr2* can enhance the phenotypes caused by elevated Nodal activity. In addition, 91% (n = 135) of embryos coinjected with 4 ng dpr2-MOs and 1.25 ng lft1-MO underwent arrest of development or died at 24 hpf, whereas this percentage was usually below 10% for single injections. Like *lft1* knockdown (Fig. 1E, right), *dpr2* knockdown rescued *shh* expression in the ventral midbrain and in the floor plate (Fig. 1E, middle) in 22 out of 23 zygotic oep^{tz257} mutants. However, *dpr2* knockdown in *MZoep* mutants,

[1]Laboratory of Developmental Biology, [2]Laboratory of Molecular Cell Biology, State Key Laboratory of Biomembrane and Membrane Biotechnology, Protein Sciences Laboratory of the Ministry of Education (MOE), Department of Biological Sciences and Biotechnology, Tsinghua University, Beijing 100084, China.

*These authors contributed equally to this work.
†To whom correspondence should be addressed. E-mail: mengam@mail.tsinghua.edu.cn (A.M.) and ygchen@mail.tsinghua.edu.cn (Y.-G.C.)